

Quantum Illumination at the Microwave Wavelengths

Shabir Barzanjeh,¹ Saikat Guha,² Christian Weedbrook,³ David Vitali,⁴ Jeffrey H. Shapiro,⁵ and Stefano Pirandola^{6,*}

¹*Institute for Quantum Information, RWTH Aachen University, 52056 Aachen, Germany*

²*Quantum Information Processing Group, Raytheon BBN Technologies, Cambridge, Massachusetts 02138, USA*

³*QKD Corp., 60 St. George St., Toronto, M5S 3G4, Canada*

⁴*School of Science and Technology, University of Camerino, Camerino, Macerata 62032, Italy*

⁵*Research Laboratory of Electronics, Massachusetts Institute of Technology, Cambridge, Massachusetts 02139, USA*

⁶*Department of Computer Science & York Centre for Quantum Technologies, University of York, York YO10 5GH, United Kingdom*

Quantum illumination is a quantum-optical sensing technique in which an entangled source is exploited to improve the detection of a low-reflectivity object that is immersed in a bright thermal background. Here we describe and analyze a system for applying this technique at microwave frequencies, a more appropriate spectral region for target detection than the optical, due to the naturally-occurring bright thermal background in the microwave regime. We use an electro-opto-mechanical converter to entangle microwave signal and optical idler fields, with the former being sent to probe the target region and the latter being retained at the source. The microwave radiation collected from the target region is then phase conjugated and upconverted into an optical field that is combined with the retained idler in a joint-detection quantum measurement. The error probability of this microwave quantum-illumination system, or quantum radar, is shown to be superior to that of any classical microwave radar of equal transmitted energy.

PACS numbers: 03.67.-a, 03.65.-w, 42.50.-p, 07.07.Df

Introduction.— Entanglement is the foundation of many quantum information protocols [1–3], but it is easily destroyed by environmental noise that, in almost all cases, kills any benefit such nonclassical correlations would otherwise have provided. Quantum illumination (QI) [4, 5], however, is a notable exception: it thrives in environments so noisy that they are entanglement breaking.

The original goal of QI was to detect the presence of a low-reflectivity object, immersed in a bright thermal background, by interrogating the target region with one optical beam while retaining its entangled counterpart for subsequent joint measurement with the light returned from that target region. Although the thermal noise destroys the entanglement, theory showed that the QI system will significantly outperform a classical (coherent-state) system of the same transmitted energy [5–7]. Later, a QI protocol was proposed for secure communication [8] whose experimental realization [9] showed that entanglement’s benefit could indeed survive an entanglement-breaking channel. Because of this feature, QI is perhaps one of the most surprising protocols for quantum sensing. Together with quantum reading [10–13], it represents a practical example of quantum channel discrimination [3], in which entanglement is beneficial for a technologically-driven information task.

So far, QI has only been demonstrated at optical wavelengths [9, 14, 15], for which naturally-occurring background radiation contains far less than one photon per mode on average, even though QI’s performance advantage *requires* the presence of a bright background. The QI communication protocol from [8, 9] deals with this

problem in a natural way by purposefully injecting amplified spontaneous emission noise to thwart eavesdropping. By contrast, similar noise injection in QI target-detection experiments has to be considered artificial, because better target-detection performance would be obtained without it. The appropriate wavelengths for QI-enabled target detection thus lie in the microwave region, in which almost all radar systems operate and in which there is naturally-occurring background radiation containing many photons per mode on average. In general, the development of quantum information techniques for microwave frequencies is quite challenging [16–18].

In this Letter, we introduce a novel QI target-detection system that operates in the microwave regime. Its transmitter uses an electro-opto-mechanical (EOM) converter [19–23] in which a mechanical resonator entangles signal and idler fields emitted from microwave and optical cavities [19, 20]. Its receiver employs another EOM device—operating as a phase-conjugator *and* a wavelength converter—whose optical output is used in a joint measurement with the retained idler. We show that our system dramatically outperforms a conventional (coherent-state) microwave radar of the same transmitted energy, achieving an orders-of-magnitude lower detection-error probability. Moreover, our system can be realized with state-of-the-art technology, and is suited to such potential applications as standoff sensing of low-reflectivity objects, and environmental scanning of electrical circuits. Thanks to its enhanced sensitivity, our system could also lead to low-flux non-invasive techniques for protein spectroscopy and biomedical imaging.

Electro-opto-mechanical converter.— As depicted in Fig. 1(a), the EOM converter couples a microwave-cavity mode (annihilation operator \hat{a}_w , frequency ω_w , damp-

* stefano.pirandola@york.ac.uk

ing rate κ_w) to an optical-cavity mode (operator \hat{a}_o , frequency ω_o , damping rate κ_o) through a mechanical resonator (operator \hat{b} , frequency ω_M , damping rate γ_M) [20–22]. In the frame rotating at the frequencies of the microwave and optical driving fields, the interaction between the cavities' photons and the resonator's phonons is governed by the Hamiltonian [24]

$$\hat{H} = \hbar\omega_M \hat{b}^\dagger \hat{b} + \hbar \sum_{j=w,o} \left[\Delta_{0,j} + g_j (\hat{b} + \hat{b}^\dagger) \right] \hat{a}_j^\dagger \hat{a}_j + \hat{H}_{\text{dri}}.$$

Here, g_j is the coupling rate between the mechanical resonator and cavity j , which is driven at frequency $\omega_j - \Delta_{0,j}$ by the coherent-driving Hamiltonian \hat{H}_{dri} [24].

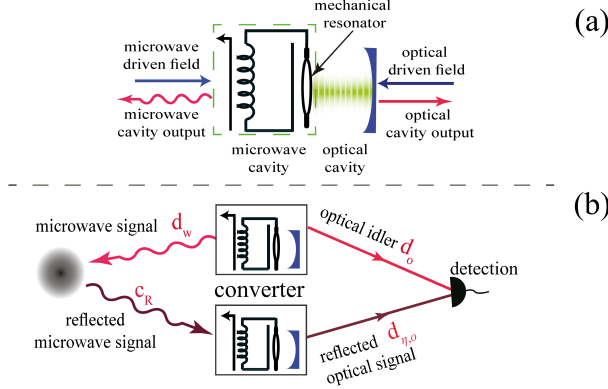


FIG. 1. (a) Schematic of the electro-opto-mechanical (EOM) converter in which driven microwave and optical cavities are coupled by a mechanical resonator. (b) Microwave-optical QI using EOM converters. The transmitter's EOM converter entangles microwave and optical fields. The receiver's EOM converter transforms the returning microwave field to the optical domain while performing a phase-conjugate operation.

The electro-opto-mechanical coupling rates g_j are typically small, so that we can linearize the Hamiltonian by expanding the cavity modes around their steady-state field amplitudes $\hat{c}_j = \hat{a}_j - \sqrt{N_j}$, where the $N_j \gg 1$ are the mean numbers of cavity photons induced by the pumps [19, 25]. In the interaction picture with respect to the free Hamiltonian, we may then write [24]

$$\hat{H} = \hbar G_o (\hat{c}_o \hat{b} + \hat{b}^\dagger \hat{c}_o^\dagger) + \hbar G_w (\hat{c}_w \hat{b}^\dagger + \hat{b} \hat{c}_w^\dagger), \quad (1)$$

where $G_j = g_j \sqrt{N_j}$ is the multi-photon coupling rate. This expression assumes that the effective cavity detunings satisfy $\Delta_w = -\Delta_o = \omega_M$ and that resonator is in its fast-oscillation regime, so that the red sideband drives the microwave cavity while the blue sideband drives the optical cavity and we can neglect terms oscillating at $\pm 2\omega_M$.

Equation (1) shows that the mechanical resonator mediates a delayed interaction between the optical and microwave cavity modes. Its first term is a parametric down-conversion interaction that entangles the mechanical resonator and the optical cavity mode. This entanglement is transmitted to the propagating optical mode \hat{d}_o , if the opto-mechanical rate G_o^2/κ_o exceeds the decoherence rate of the mechanical resonator

$r = \gamma_M \bar{n}_b^T \approx \gamma_M k_B T_{\text{EOM}} / \hbar\omega_M$, where k_B is Boltzmann's constant, T_{EOM} is the EOM converter's absolute temperature, $\bar{n}_b^T = [e^{\hbar\omega_M / (k_B T_{\text{EOM}})} - 1]^{-1}$, and the approximation presumes $k_B T_{\text{EOM}} \gg \hbar\omega_M$, as will be the case for the parameter values assumed later. The second term in Eq. (1) is a beam-splitter interaction between the mechanical resonator and the microwave cavity mode that transfers the entanglement to the propagating microwave field \hat{d}_w , as long as the microwave-mechanical rate satisfies $G_w^2/\kappa_w > r$ [25, 26].

Microwave-optical entanglement.— The output propagating modes can be expressed in terms of the intracavity quantum noise operators, $\hat{c}_{j,\text{in}}$, and the quantum Brownian noise operator, \hat{b}_{int} , via [24]

$$\hat{d}_w = A_w \hat{c}_{w,\text{in}} - B \hat{c}_{o,\text{in}}^\dagger - C_w \hat{b}_{\text{int}}, \quad (2)$$

$$\hat{d}_o = B \hat{c}_{w,\text{in}}^\dagger + A_o \hat{c}_{o,\text{in}} - C_o \hat{b}_{\text{int}}^\dagger, \quad (3)$$

where A_j , B , and C_j depend on the cooperativity terms $\Gamma_j = G_j^2/\kappa_j\gamma_M$ as given in [24]. The $\hat{c}_{w,\text{in}}$, $\hat{c}_{o,\text{in}}$ and \hat{b}_{int} modes in Eqs. (2) and (3) are in independent thermal states whose average photon numbers, \bar{n}_w^T , \bar{n}_o^T , and \bar{n}_b^T , are given by temperature- T_{EOM} Planck laws at their respective frequencies. It follows that the propagating modes, \hat{d}_w and \hat{d}_o , are in a zero-mean, jointly-Gaussian state completely characterized by the second moments,

$$\bar{n}_w \equiv \langle \hat{d}_w^\dagger \hat{d}_w \rangle = |A_w|^2 \bar{n}_w^T + |B|^2 (\bar{n}_o^T + 1) + |C_w|^2 \bar{n}_b^T,$$

$$\bar{n}_o \equiv \langle \hat{d}_o^\dagger \hat{d}_o \rangle = |B|^2 (\bar{n}_w^T + 1) + |A_o|^2 \bar{n}_o^T + |C_o|^2 (\bar{n}_b^T + 1),$$

$$\langle \hat{d}_w \hat{d}_o \rangle = A_w B (\bar{n}_w^T + 1) - B A_o \bar{n}_o^T + C_w C_o (\bar{n}_b^T + 1).$$

The propagating microwave and optical fields will be entangled if and only if the metric $\mathcal{E} \equiv |\langle \hat{d}_w \hat{d}_o \rangle| / \sqrt{\bar{n}_w \bar{n}_o}$ is greater than 1 [24]. As we can see from Fig. 2, there is a wide region where $\mathcal{E} > 1$ in the plane of the cooperativity parameters, Γ_w and Γ_o , varied by varying the microwave and optical powers driving their respective cavities, and assuming experimentally-achievable system parameters [25, 27]. The threshold condition $\mathcal{E} = 1$ almost coincides with the boundary between the stable and unstable parameter regions, as given by the Routh-Hurwitz criterion [33].

The quality of our microwave-optical source can also be evaluated using measures of quantum correlations, as typical in quantum information. Since the QI's advantage is computed at fixed mean number of microwave photons \bar{n}_w irradiated through the target, the most powerful quantum resources are expected to be those maximizing their quantum correlations per microwave photon emitted. Following this physical intuition, we analyze our source in terms of the normalized log-negativity [28] E_N/\bar{n}_w and the normalized coherent information [29, 30] $I(o|w)/\bar{n}_w$. Respectively, they represent an upper and a lower bound to the mean number of entanglement bits (ebits) which are distillable for each microwave photon emitted by the source [24]. Furthermore, since our source is in a mixed state (more precisely, a two-mode squeezed

thermal state), we also quantify its normalized quantum discord [24, 31] $D(w|o)/\bar{n}_w$, which captures the quantum correlations carried by each microwave photon. As we can see from Fig. 2, our source has a remarkable performance in producing distillable ebits and discordant bits for each microwave photon emitted.

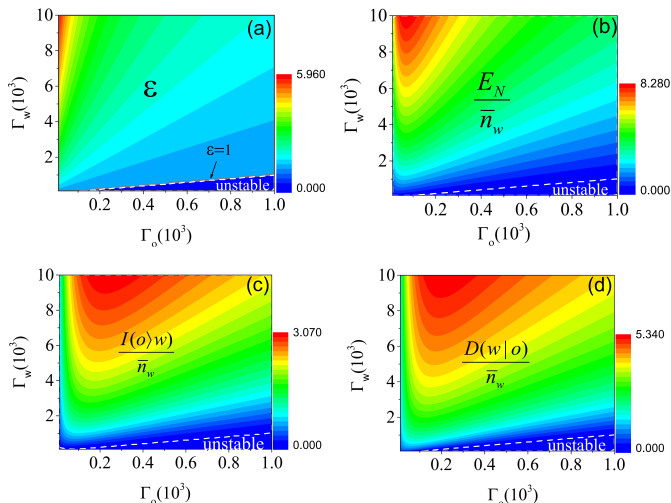


FIG. 2. Performance of our microwave-optical source versus the cooperativity parameters Γ_w and Γ_o . We show the behaviour of the entanglement metric \mathcal{E} (abstract units) in panel (a), the normalized logarithmic negativity E_N/\bar{n}_w (ebits per microwave photon) in panel (b), the normalized coherent information $I(o|w)/\bar{n}_w$ (qubits per microwave photon) in panel (c), and the normalized quantum discord $D(w|o)/\bar{n}_w$ (discordant bits per microwave photon) in panel (d). In all panels we assume experimentally-achievable parameters [25, 27]: a 10-ng-mass mechanical resonator with $\omega_M/2\pi = 10$ MHz and $Q = 30 \times 10^3$; a microwave cavity with $\omega_w/2\pi = 10$ GHz and $\kappa_w = 0.2\omega_M$; and a 1-mm-long optical cavity with $\kappa_o = 0.1\omega_M$ driven by a 1064-nm-wavelength laser. The opto-mechanical and electro-mechanical coupling rates are $g_o/2\pi = 115.512$ Hz and $g_w/2\pi = 0.327$ Hz, and the entire EOM converter is held at temperature $T_{\text{EOM}} = 30$ mK. In each panel, the boundary between stable and unstable operation was obtained from the Routh-Hurwitz criterion [33].

Microwave quantum illumination.— For QI target detection, our signal-idler mode pair analysis must be extended to a continuous-wave EOM converter whose W_m -Hz-bandwidth [32] output fields are used in a t_m -seconduration measurement involving $M = t_m W_m \gg 1$ independent, identically-distributed (iid) mode pairs. The M signal modes interrogate the target region that is equally likely to contain (hypothesis H_1) or not contain (hypothesis H_0) a low-reflectivity object. Either way, the microwave field that is returned consists of M iid modes. Using \hat{c}_R to denote the annihilation operator for the mode returned from transmission of \hat{d}_w , we have that $\hat{c}_R = \hat{c}_B$ under hypothesis H_0 , and $\hat{c}_R = \sqrt{\eta}\hat{d}_w + \sqrt{1-\eta}\hat{c}_B$, under hypothesis H_1 . Here, $0 < \eta \ll 1$ is the roundtrip transmitter-to-target-to-receiver transmissivity (including propagation losses and target reflectivity), and the background-noise mode, \hat{c}_B ,

is in a thermal state with temperature- T_B Planck-law average photon number \bar{n}_B under H_0 , and in a thermal state with $\bar{n}_B/(1-\eta) \approx \bar{n}_B$ under H_1 [5]. See Fig. 1(b).

Under H_1 , the returned microwave and the retained optical fields are in a zero-mean, jointly-Gaussian state with a nonzero phase-sensitive cross correlation $\langle \hat{c}_R \hat{d}_o \rangle$ that is invariant to the \bar{n}_B value, while $\langle \hat{c}_R^\dagger \hat{c}_R \rangle$ increases with increasing \bar{n}_B . Consequently, the returned and retained radiation under H_1 will *not* be entangled when

$$\bar{n}_B \geq \bar{n}_B^{\text{thresh}} \equiv \eta \left(|\langle \hat{d}_w \hat{d}_o \rangle|^2 / \bar{n}_o - \bar{n}_w \right).$$

Microwave-to-optical phase-conjugate receiver.— The receiver passes the M return modes into the microwave cavity of another (identical) EOM converter to produce M iid optical-output modes each given by $\hat{d}_{\eta,o} = B\hat{c}_R^\dagger + A_o\hat{c}'_{o,\text{in}} - C_o\hat{b}'_{\text{int}}^\dagger$, where $\{\hat{c}'_{w,\text{in}}, \hat{c}'_{o,\text{in}}, \hat{b}'_{\text{int}}\}$ have the same states as their counterparts in the transmitter's EOM converter. The receiver's EOM converter thus phase conjugates the returned microwave field *and* upconverts it to an optical field. This output is combined with the retained idler on a 50–50 beam splitter whose outputs are photodetected and their photon counts—over the t_m -second measurement interval—are subtracted to yield an outcome from which a minimum error-probability decision about object absence or presence will be made [6]. For $M \gg 1$, the resulting error probability is [6, 24]

$$P_{\text{QI}}^{(M)} = \text{erfc} \left(\sqrt{\text{SNR}_{\text{QI}}^{(M)}} / 8 \right) / 2, \text{ with } \text{SNR}_{\text{QI}}^{(M)} \text{ being the QI system's signal-to-noise ratio for its } M \text{ mode pairs [24] and } \text{erfc}(\dots) \text{ being the complementary error function [6].}$$

Comparison with classical microwave transmitters.— Suppose that a coherent-state microwave transmitter—emitting $M\bar{n}_w$ photons on average, with \bar{n}_w equaling the mean number of microwave photons per mode emitted by our source—is used to assess target absence or presence. Homodyne detection of the microwave field returned from the target region followed by minimum error-probability processing of its output results in an error probability [6]

$$P_{\text{coh}}^{(M)} = \text{erfc} \left(\sqrt{\text{SNR}_{\text{coh}}^{(M)}} / 8 \right) / 2, \text{ in terms of this sys-}$$

tem's signal-to-noise ratio, $\text{SNR}_{\text{coh}}^{(M)} = 4\eta M\bar{n}_w / (2\bar{n}_B + 1)$. This performance approximates the error exponent of the quantum Chernoff bound [35–37] computed for $M \gg 1$, implying that homodyne detection is the asymptotically optimal receiver for target detection when a coherent-state transmitter is employed.

Figure 3 plots $P_{\text{QI}}^{(M)}$ and $P_{\text{coh}}^{(M)}$ versus $\log_{10} M$ for the EOM converter parameters given in Fig. 2 and $\eta = 0.07$. It assumes $\Gamma_w = 5181.95$ and $\Gamma_o = 668.43$ (implying $\bar{n}_w = 0.739$ and $\bar{n}_o = 0.681$) and $T_B = 293$ K (implying $\bar{n}_B = 610$). We see that the QI system can have an error probability that is orders of magnitude lower than that of the coherent-state system. Moreover, according to Ref. [5], no other classical-state system with the same energy constraint can have a lower error probability than the coherent-state system.

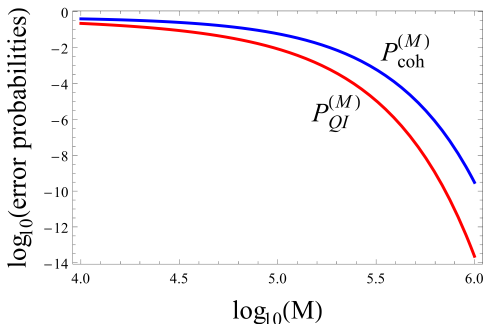


FIG. 3. $P_{\text{QI}}^{(M)}$ and $P_{\text{coh}}^{(M)}$ versus the time-bandwidth product, M , assuming $\eta = 0.07$, $\Gamma_w = 5181.95$ and $\Gamma_o = 668.43$ (implying $\bar{n}_w = 0.739$ and $\bar{n}_o = 0.681$), and room temperature $T_B = 293$ K (implying $\bar{n}_B = 610 \gg \bar{n}_B^{\text{thresh}} = 0.069$).

To further study the performance gain of our microwave QI system over a classical sensor, we evaluate $\mathcal{F} \equiv \text{SNR}_{\text{QI}}^{(M)} / \text{SNR}_{\text{coh}}^{(M)}$ for large M . This figure of merit depends on the cooperativity parameters, Γ_w and Γ_o , whose values are typically large $\Gamma_j \gg 1$ (cf. the values in Fig. 2, which rely on experimentally-achievable parameters) and the brightness of the background, \bar{n}_B . As shown in Fig. 4, QI's superiority prevails in a substantial region of Γ_w , Γ_o values corresponding to Fig. 2 regions where our source has the best efficiency in producing quantum entanglement and, more generally, quantum correlations, per microwave photon emitted. Such advantage is found as long as the average number of microwave photons is sufficiently low.

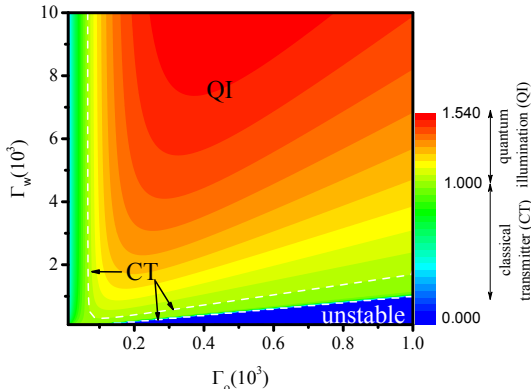


FIG. 4. QI-advantage figure of merit, \mathcal{F} , versus Γ_w and Γ_o . For $\mathcal{F} > 1$, the QI system has lower error probability than any classical-state system, i.e., classical transmitter (CT), of the same transmitted energy. See Fig. 2 for the other parameter values.

Conclusion and Discussion.— We have shown that quantum illumination can be performed in its more natural setting for target detection, i.e., the microwave regime, by using a pair of electro-opto-mechanical converters. Thanks to this converter, the target region can be interrogated at a microwave frequency, while the

quantum-illumination joint measurement needed for target detection is made at optical frequency, where the high-performance photodetectors needed to obtain QI's performance advantage are available.

An optimized EOM converter is able to generate strong quantum entanglement and quantum correlations between its microwave and optical outputs. These correlations can successfully be exploited for target detection, yielding lower error probability than that of any classical-state microwave system of the same transmitted energy. The QI advantage is especially evident when detecting the faint returns from low-reflectivity objects embedded in the bright thermal noise typical of room-temperature microwave environments.

Note that we assumed unit quantum efficiency for the optical part of our quantum receiver. This is not far from current experimental conditions: photon collection efficiencies from optical cavities can be very high ($> 74\%$ in Ref. [38]), loss at the beam splitter can be extremely low, and photodetection can be extremely efficient at optical wavelengths. Thus the main source of loss may come from the optical storage of the idler mode, to be preserved during the signal roundtrip time. This is not an issue for short-range applications but, for long-range tasks, the idler loss must remain below 3 dB, otherwise the QI advantage of the phase-conjugating quantum receiver is lost [6]. While using a good quantum memory (e.g., a rare-earth doped-crystal [39]) would solve the problem, the practical solution of storing the idler into an optical-fiber delay line would restrict the maximum range of the quantum radar to about 11.25 km in free-space (assuming a fiber loss of 0.2 dB/km and fiber propagation speed equal to $2c/3$, where c is vacuum light-speed).

Finally, extending our results to lower frequencies (below 1 GHz), our scheme could potentially be used for non-invasive NMR spectroscopy in structural biology (structure of proteins and nucleic acids) and in medical applications (magnetic resonance imaging). Future implementations of quantum illumination at the microwave regime could also be achieved by using other quantum sources, for instance based on Josephson parametric amplifiers, which are able to generate entangled microwave modes of high quality [40–43]. These amplifiers might become a very good choice once that suitable high-performance microwave photo-detectors are made available.

Acknowledgments.— S.B. is grateful for support from the Alexander von Humboldt foundation. D.V. is sponsored by the European Commission (ITN-Marie Curie Project ‘cQOM’, Grant No. 290161, and FET-Open Project ‘iQUOEMS’, Grant No. 323924). S.G. was supported by the US Office of Naval Research contract number N00014-14-C-0002. J.H.S. appreciates sponsorship by AFOSR and ONR. S.P. has been sponsored by a Leverhulme Trust research fellowship (‘qBIO’) and EPSRC via ‘qDATA’ (Grant no. EP/L011298/1) and ‘HIPER-COM’ (Grant No. EP/J00796X/1).

- [1] M. A. Nielsen and I. L. Chuang, *Quantum Computation and Quantum Information* (Cambridge Univ. Press, 2000).
- [2] M. M. Wilde, *Quantum Information Theory*, (Cambridge Univ. Press, 2013).
- [3] C. Weedbrook, S. Pirandola, R. García-Patrón, N. J. Cerf, T. C. Ralph, J. H. Shapiro, and S. Lloyd, *Rev. Mod. Phys.* **84**, 621 (2012).
- [4] S. Lloyd, *Science* **321**, 1463 (2008).
- [5] S.-H. Tan, B. I. Erkmen, V. Giovannetti, S. Guha, S. Lloyd, L. Maccone, S. Pirandola, and J. H. Shapiro, *Phys. Rev. Lett.* **101**, 253601 (2008).
- [6] S. Guha and B. I. Erkmen, *Phys. Rev. A* **80**, 052310 (2009).
- [7] C. Weedbrook, S. Pirandola, J. Thompson, V. Vedral, and M. Gu, arXiv:1312.3332 [quant-ph].
- [8] J. H. Shapiro, *Phys. Rev. A* **80**, 022320 (2009).
- [9] Z. Zhang, M. Tengner, T. Zhong, F. N. C. Wong, and J. H. Shapiro, *Phys. Rev. Lett.* **111**, 010501 (2013).
- [10] S. Pirandola, *Phys. Rev. Lett.* **106**, 090504 (2011).
- [11] S. Pirandola, C. Lupo, V. Giovannetti, S. Mancini, and S. L. Braunstein, *New J. Phys.* **13**, 113012 (2011).
- [12] G. Spedalieri, C. Lupo, S. Mancini, S. L. Braunstein, and S. Pirandola, *Phys. Rev. A* **86**, 012315 (2012).
- [13] C. Lupo, S. Pirandola, V. Giovannetti, and S. Mancini, *Phys. Rev. A* **87**, 062310 (2013).
- [14] E. D. Lopaeva, I. Ruo Berchera, I. P. Degiovanni, S. Olivares, G. Brida, and M. Genovese, *Phys. Rev. Lett.* **110**, 153603 (2013).
- [15] Z. Zhang, S. Mouradian, F. N. C. Wong, and J. H. Shapiro, arXiv:1411.5969 [quant-ph].
- [16] C. Weedbrook, S. Pirandola, S. Lloyd, and T. C. Ralph, *Phys. Rev. Lett.* **105**, 110501 (2010).
- [17] C. Weedbrook, S. Pirandola, and T. C. Ralph, *Phys. Rev. A* **86**, 022318 (2012).
- [18] C. Weedbrook, C. Ottaviani, and S. Pirandola, *Phys. Rev. A* **89**, 012309 (2014).
- [19] Sh. Barzanjeh, D. Vitali, P. Tombesi, and G. J. Milburn, *Phys. Rev. A* **84**, 042342 (2011).
- [20] Sh. Barzanjeh, M. Abdi, G. J. Milburn, P. Tombesi, and D. Vitali, *Phys. Rev. Lett.* **109**, 130503 (2012).
- [21] R. W. Andrews, R. W. Peterson, T. P. Purdy, K. Cicak, R. W. Simmonds, C. A. Regal, and K. W. Lehnert, *Nature Phys.* **10**, 321 (2014).
- [22] J. Bochmann, A. Vainsencher, D. D. Awschalom, and A. N. Cleland, *Nature Phys.* **9**, 712 (2013).
- [23] T. Bagci, A. Simonsen, S. Schmid, L. G. Villanueva, E. Zeuthen, J. Appel, J. M. Taylor, A. Sørensen, A. Schliesser, and E. S. Polzik, *Nature* **507**, 81 (2014).
- [24] See Supplemental Material for more details. We provide technical details on the following: (i) Hamiltonian of an electro-opto-mechanical system, (ii) linearization of the Hamiltonian, (iii) derivation of the quantum Langevin equations with internal losses, (iv) study of the microwave-optical entanglement considering the entanglement metric, the logarithmic negativity and the coherent information, (v) general study of the quantum correlations as quantified by quantum discord, and (vi) analysis of the error probability for M mode pairs.
- [25] T. A. Palomaki, J. D. Teufel, R. W. Simmonds, and K. W. Lehnert, *Science* **342**, 710 (2013).
- [26] S. G. Hofer, W. Wieczorek, M. Aspelmeyer, and K. Hammerer, *Phys. Rev. A* **84**, 052327 (2011).
- [27] T. A. Palomaki, J. W. Harlow, J. D. Teufel, R. W. Simmonds, and K. W. Lehnert, *Nature* **495**, 210 (2013).
- [28] J. Eisert, Ph.D. thesis, University of Potsdam, 2001; G. Vidal and R. F. Werner, *Phys. Rev. A* **65**, 032314 (2002); M.B. Plenio, *Phys. Rev. Lett.* **95**, 090503 (2005).
- [29] B. Schumacher and M.A. Nielsen, *Phys. Rev. A* **54**, 2629 (1996).
- [30] S. Lloyd, *Phys. Rev. A* **55**, 1613 (1997).
- [31] S. Pirandola, G. Spedalieri, S. L. Braunstein, N. J. Cerf, and S. Lloyd, *Phys. Rev. Lett.* **113**, 140405 (2014).
- [32] The common bandwidth of the entangled microwave and optical fields is $W_m = \gamma_M(\Gamma_w - \Gamma_o + 1)$, in terms of the resonator's damping rate and the cooperativity parameters.
- [33] The system is stable if the Routh-Hurwitz criterion is satisfied. For $\Gamma_i \gg 0$, this criterion reduces to the following necessary and sufficient condition [34]:
- $$\kappa_w \Gamma_w - \kappa_o \Gamma_o > \tilde{K} \max \left\{ \kappa_w - \kappa_o, \frac{\kappa_o^2 - \kappa_w^2}{2\gamma_M + \kappa_w + \kappa_o} \right\},$$
- where $\tilde{K} = \Gamma_w(1 + \kappa_o/\kappa_w)^{-1} + \Gamma_o(1 + \kappa_w/\kappa_o)^{-1}$.
- [34] Y.-D. Wang and A. A. Clerk, *Phys. Rev. Lett.* **110**, 253601 (2013).
- [35] K. M. R. Audenaert, J. Calsamiglia, L. Masanes, R. Muñoz-Tapia, A. Acín, E. Bagan, and F. Verstraete, *Phys. Rev. Lett.* **98**, 160501 (2007).
- [36] K. M. R. Audenaert, M. Nussbaum, A. Szkola, and F. Verstraete, *Commun. Math. Phys.* **279**, 251 (2008).
- [37] S. Pirandola, and S. Lloyd, *Phys. Rev. A* **78**, 012331 (2008).
- [38] A. Reiserer, S. Ritter, and G. Rempe, *Science* **342**, 1349 (2013).
- [39] M. Zhong *et al.*, *Nature* **517**, 177 (2015).
- [40] M. A. Castellanos-Beltran and K. W. Lehnert, *Appl. Phys. Lett.* **91**, 083509 (2007).
- [41] N. Bergeal *et al.*, *Nature (London)* **465**, 64 (2010).
- [42] N. Roch, E. Flurin, F. Nguyen, P. Morfin, P. Campagne-Ibarcq, M. H. Devoret, and B. Huard, *Phys. Rev. Lett.* **108**, 147701 (2012).
- [43] C. Eichler, Y. Salathe, J. Mlynek, S. Schmidt, and A. Wallraff, *Phys. Rev. Lett.* **113**, 110502 (2014).

Supplemental Material

Contents. In this Supplemental Material we provide technical details on the following: (i) Hamiltonian of an electro-opto-mechanical system, (ii) linearization of the Hamiltonian, (iii) derivation of the quantum Langevin equations with internal losses, (iv) study of the microwave-optical entanglement considering the entanglement metric, the logarithmic negativity and the coherent information, (v) general study of the quantum correlations as quantified by quantum discord, and (vi) analysis of the error probability for M mode pairs.

I. HAMILTONIAN OF AN ELECTRO-OPTO-MECHANICAL SYSTEM

Our electro-opto-mechanical (EOM) converter consists of a mechanical resonator (MR) that is capacitively coupled on one side to a driven superconducting microwave cavity, and on the other side to a driven Fabry-Pérot optical cavity [S1–S3]. These cavities' driving fields are at radian frequencies $\omega_{d,j} = \omega_j - \Delta_{0,j}$, where the $\Delta_{0,j}$ are the detunings from their resonant frequencies ω_j , with $j = w, o$ denoting the microwave and optical cavities, respectively. We include intrinsic losses for these cavities with rates κ_j^{int} , and use κ_j^{in} to denote their input-port coupling rates. The Hamiltonian of the coupled system in terms of annihilation and creation operators has been studied in Ref. [S4], and is given by

$$\begin{aligned} \hat{H} = & \hbar\omega_M \hat{b}^\dagger \hat{b} + \hbar \sum_{j=w,o} \omega_j \hat{a}_j^\dagger \hat{a}_j + \frac{\hbar g_w}{2} (\hat{b}^\dagger + \hat{b})(\hat{a}_w + \hat{a}_w^\dagger)^2 + \hbar g_o (\hat{b}^\dagger + \hat{b}) \hat{a}_o^\dagger \hat{a}_o \\ & + i\hbar E_w (e^{i\omega_{d,w}t} - e^{-i\omega_{d,w}t})(\hat{a}_w + \hat{a}_w^\dagger) + i\hbar E_o (\hat{a}_o^\dagger e^{-i\omega_{d,o}t} - \hat{a}_o e^{i\omega_{d,o}t}). \end{aligned} \quad (4)$$

Here, \hat{b} is the annihilation operator of the MR whose resonant frequency is ω_M , \hat{a}_j is the annihilation operator for cavity j whose coupling rate to the MR is g_j . The optical-driving strength is $E_o = \sqrt{2P_o \kappa_o^{\text{in}} / \hbar \omega_{d,o}}$, where P_o is the laser power. The microwave cavity is driven by an electric potential with $e(t) = -i\sqrt{2\hbar\omega_w L} E_w (e^{i\omega_{d,w}t} - e^{-i\omega_{d,w}t})$ where L is the inductance in the microwave electric circuit and E_w describes the amplitude of the microwave driving field [S4]. In writing Eq. (4) we have ignored any additional degenerate modes that the optical and microwave cavities might have. Ignoring such modes is justified whenever scattering of photons from the driven mode into other cavity modes can be neglected. That condition prevails, for example, with short cavities whose free spectral ranges greatly exceed the MR's resonant frequency, thus ensuring that only one mode from each cavity interacts with the MR, and that adjacent modes are not excited by the driving fields.

In the interaction picture with respect to $\hbar\omega_{d,w} \hat{a}_w^\dagger \hat{a}_w + \hbar\omega_{d,o} \hat{a}_o^\dagger \hat{a}_o$, and neglecting terms oscillating at $\pm 2\omega_{d,w}$, the system Hamiltonian reduces to

$$\hat{H} = \hbar\omega_M \hat{b}^\dagger \hat{b} + \hbar \sum_{j=w,o} \left[\Delta_{0,j} + g_j (\hat{b}^\dagger + \hat{b}) \right] \hat{a}_j^\dagger \hat{a}_j + \hat{H}_{\text{dri}}, \quad (5)$$

where the Hamiltonian associated with the driving fields is $\hat{H}_{\text{dri}} = i\hbar \sum_{j=w,o} E_j (\hat{a}_j^\dagger - \hat{a}_j)$.

II. LINEARIZATION OF THE HAMILTONIAN

We can linearize Hamiltonian (5) by expanding the cavity modes around their steady-state field amplitudes, $\hat{c}_j = \hat{a}_j - \sqrt{N_j}$, where $N_j = |E_j|^2 / (\kappa_j^2 + \Delta_j^2) \gg 1$ is the mean number of intracavity photons induced by the microwave or optical pumps [S4], the $\kappa_j = \kappa_j^{\text{in}} + \kappa_j^{\text{int}}$ are the total cavity decay rates, and the Δ_j are the effective cavity detunings. It is then convenient to move to the interaction picture with respect to the free Hamiltonian, $\hbar\omega_M \hat{b}^\dagger \hat{b} + \hbar \sum_{j=w,o} \omega_j \hat{a}_j^\dagger \hat{a}_j$, where the linearized Hamiltonian becomes

$$\hat{H} = \hbar \sum_{j=w,o} G_j (\hat{b} e^{-i\omega_M t} + \hat{b}^\dagger e^{i\omega_M t}) (\hat{c}_j^\dagger e^{i\Delta_j t} + \hat{c}_j e^{-i\Delta_j t}), \quad (6)$$

where $G_j = g_j \sqrt{N_j}$. By setting the effective cavity detunings so that $\Delta_w = -\Delta_o = \omega_M$ and neglecting the terms rotating at $\pm 2\omega_M$, the above Hamiltonian reduces to

$$\hat{H} = \hbar G_o (\hat{c}_o \hat{b} + \hat{b}^\dagger \hat{c}_o^\dagger) + \hbar G_w (\hat{c}_w \hat{b}^\dagger + \hat{b} \hat{c}_w^\dagger), \quad (7)$$

as specified in the paper.

III. QUANTUM LANGEVIN EQUATIONS WITH INTERNAL LOSSES

The full quantum treatment of the system can be given in terms of the quantum Langevin equations in which we add to the Heisenberg equations the quantum noise acting on the mechanical resonator (\hat{b}_{int} with damping rate γ_M), as well as the cavities' input fluctuations ($\hat{c}_{j, \text{in}}$, for $j = w, o$, with rates κ_j^{in}), plus the intrinsic losses of the cavity modes ($\hat{c}_{j, \text{int}}$, for $j = w, o$, with loss rates κ_j^{int}). These noises have the correlation functions

$$\langle \hat{c}_{j, \text{in}}(t) \hat{c}_{j, \text{in}}^\dagger(t') \rangle = \langle \hat{c}_{j, \text{in}}^\dagger(t) \hat{c}_{j, \text{in}}(t') \rangle + \delta(t - t') = (\bar{n}_j^T + 1) \delta(t - t'), \quad (8a)$$

$$\langle \hat{c}_{j, \text{int}}(t) \hat{c}_{j, \text{int}}^\dagger(t') \rangle = \langle \hat{c}_{j, \text{int}}^\dagger(t) \hat{c}_{j, \text{int}}(t') \rangle + \delta(t - t') = (\bar{n}_j^{\text{int}} + 1) \delta(t - t'), \quad (8b)$$

$$\langle \hat{b}_{\text{int}}(t) \hat{b}_{\text{int}}^\dagger(t') \rangle = \langle \hat{b}_{\text{int}}^\dagger(t) \hat{b}_{\text{int}}(t') \rangle + \delta(t - t') = (\bar{n}_b^T + 1) \delta(t - t'), \quad (8c)$$

where \bar{n}_j^{int} , \bar{n}_j^T , and \bar{n}_b^T are the Planck-law thermal occupancies of each bath. The resulting Langevin equations for the cavity modes and MR are

$$\dot{\hat{c}}_w = -\kappa_w \hat{c}_w - iG_w \hat{b} + \sqrt{2\kappa_w^{\text{in}}} \hat{c}_{w, \text{in}} + \sqrt{2\kappa_w^{\text{int}}} \hat{c}_{w, \text{int}}, \quad (9a)$$

$$\dot{\hat{c}}_o = -\kappa_o \hat{c}_o - iG_o \hat{b}^\dagger + \sqrt{2\kappa_o^{\text{in}}} \hat{c}_{o, \text{in}} + \sqrt{2\kappa_o^{\text{int}}} \hat{c}_{o, \text{int}}, \quad (9b)$$

$$\dot{\hat{b}} = -\gamma_M \hat{b} - iG_o \hat{c}_o^\dagger - iG_w \hat{c}_w + \sqrt{2\gamma_M} \hat{b}_{\text{int}}. \quad (9c)$$

We can solve the above equations in the Fourier domain to obtain the microwave and optical cavities' variables. By substituting the solutions of Eqs. (9a)–(9c) into the corresponding input-output formula for the cavities' variables, i.e., $\hat{d}_j \equiv \hat{c}_{j, \text{out}} = \sqrt{2\kappa_j^{\text{in}}} \hat{c}_j - \hat{c}_{j, \text{in}}$, we obtain

$$\hat{d}_w = A_w(\omega) \hat{c}_{w, \text{in}} - B(\omega) \hat{c}_{o, \text{in}}^\dagger - C_w(\omega) \hat{b}_{\text{int}} - D_w(\omega) \hat{c}_{o, \text{int}}^\dagger - E_w(\omega) \hat{c}_{w, \text{int}}, \quad (10a)$$

$$\hat{d}_o = A_o(\omega) \hat{c}_{o, \text{in}} + B^*(\omega) \hat{c}_{w, \text{in}}^\dagger - C_o(\omega) \hat{b}_{\text{int}}^\dagger + D_o(\omega) \hat{c}_{w, \text{int}}^\dagger + E_o(\omega) \hat{c}_{o, \text{int}}, \quad (10b)$$

where

$$A_w(\omega) = \frac{[\tilde{\omega}_w - 2\kappa_w^{\text{in}}/\kappa_w][\Gamma_o - \tilde{\omega}_o \tilde{\omega}_b] - \Gamma_w \tilde{\omega}_o}{\tilde{\omega}_w [\tilde{\omega}_o \tilde{\omega}_b - \Gamma_o] + \Gamma_w \tilde{\omega}_o}, \quad (11a)$$

$$A_o(\omega) = \frac{-[\tilde{\omega}_o^* - 2\kappa_o^{\text{in}}/\kappa_o][\Gamma_w + \tilde{\omega}_w^* \tilde{\omega}_b^*] + \Gamma_o \tilde{\omega}_w^*}{\tilde{\omega}_w^* [\tilde{\omega}_o^* \tilde{\omega}_b^* - \Gamma_o] + \Gamma_w \tilde{\omega}_o^*}, \quad (11b)$$

$$B(\omega) = 2\sqrt{\frac{\kappa_o^{\text{in}}}{\kappa_o}} \sqrt{\frac{\kappa_w^{\text{in}}}{\kappa_w}} \frac{\sqrt{\Gamma_w \Gamma_o}}{\tilde{\omega}_w [\tilde{\omega}_o \tilde{\omega}_b - \Gamma_o] + \Gamma_w \tilde{\omega}_o}, \quad (11c)$$

$$C_w(\omega) = \sqrt{\frac{\kappa_w^{\text{in}}}{\kappa_w}} \frac{2i\sqrt{\Gamma_w} \tilde{\omega}_o}{\tilde{\omega}_w [\tilde{\omega}_o \tilde{\omega}_b - \Gamma_o] + \Gamma_w \tilde{\omega}_o}, \quad (11d)$$

$$C_o(\omega) = \sqrt{\frac{\kappa_o^{\text{in}}}{\kappa_o}} \frac{2i\sqrt{\Gamma_o} \tilde{\omega}_w^*}{\tilde{\omega}_w^* [\tilde{\omega}_o^* \tilde{\omega}_b^* - \Gamma_o] + \Gamma_w \tilde{\omega}_o^*}, \quad (11e)$$

$$D_w(\omega) = 2\sqrt{\frac{\kappa_o^{\text{int}}}{\kappa_o}} \sqrt{\frac{\kappa_w^{\text{in}}}{\kappa_w}} \frac{\sqrt{\Gamma_o \Gamma_w}}{\tilde{\omega}_w [\tilde{\omega}_o \tilde{\omega}_b - \Gamma_o] + \Gamma_w \tilde{\omega}_o}, \quad (11f)$$

$$D_o(\omega) = 2\sqrt{\frac{\kappa_o^{\text{in}}}{\kappa_o}} \sqrt{\frac{\kappa_w^{\text{int}}}{\kappa_w}} \frac{\sqrt{\Gamma_o \Gamma_w}}{\tilde{\omega}_w^* [\tilde{\omega}_o^* \tilde{\omega}_b^* - \Gamma_o] + \Gamma_w \tilde{\omega}_o^*}, \quad (11g)$$

$$E_w(\omega) = 2\sqrt{\frac{\kappa_w^{\text{int}}}{\kappa_w}} \sqrt{\frac{\kappa_o^{\text{in}}}{\kappa_o}} \frac{\Gamma_o - \tilde{\omega}_o \tilde{\omega}_b}{\tilde{\omega}_w [\tilde{\omega}_o \tilde{\omega}_b - \Gamma_o] + \Gamma_w \tilde{\omega}_o}, \quad (11h)$$

$$E_o(\omega) = 2\sqrt{\frac{\kappa_o^{\text{int}}}{\kappa_o}} \sqrt{\frac{\kappa_w^{\text{in}}}{\kappa_w}} \frac{\Gamma_w + \tilde{\omega}_w^* \tilde{\omega}_b^*}{\tilde{\omega}_w^* [\tilde{\omega}_o^* \tilde{\omega}_b^* - \Gamma_o] + \Gamma_w \tilde{\omega}_o^*}, \quad (11i)$$

with $\tilde{\omega}_j = 1 - i\omega/\kappa_j$, $\tilde{\omega}_b = 1 - i\omega/\gamma_M$, and $\Gamma_j = G_j^2/\kappa_j\gamma_M$. The coefficients (11a)–(11i) become much simpler at $\omega \simeq 0$, which corresponds to take a narrow frequency band around each cavity resonance, viz.,

$$A_w = \frac{[1 - 2\kappa_w^{\text{in}}/\kappa_w][\Gamma_o - 1] - \Gamma_w}{1 - \Gamma_o + \Gamma_w}, \quad (12a)$$

$$A_o = \frac{-[1 - 2\kappa_o^{\text{in}}/\kappa_o][\Gamma_w + 1] + \Gamma_o}{1 - \Gamma_o + \Gamma_w}, \quad (12b)$$

$$B = 2\sqrt{\frac{\kappa_o^{\text{in}}}{\kappa_o}} \sqrt{\frac{\kappa_w^{\text{in}}}{\kappa_w}} \frac{\sqrt{\Gamma_w\Gamma_o}}{1 - \Gamma_o + \Gamma_w}, \quad (12c)$$

$$C_w = \sqrt{\frac{\kappa_w^{\text{in}}}{\kappa_w}} \frac{2i\sqrt{\Gamma_w}}{1 - \Gamma_o + \Gamma_w}, \quad (12d)$$

$$C_o = \sqrt{\frac{\kappa_o^{\text{in}}}{\kappa_o}} \frac{2i\sqrt{\Gamma_o}}{1 - \Gamma_o + \Gamma_w}, \quad (12e)$$

$$D_w = 2\sqrt{\frac{\kappa_o^{\text{int}}}{\kappa_o}} \sqrt{\frac{\kappa_w^{\text{in}}}{\kappa_w}} \frac{\sqrt{\Gamma_o\Gamma_w}}{1 - \Gamma_o + \Gamma_w}, \quad (12f)$$

$$D_o = 2\sqrt{\frac{\kappa_o^{\text{in}}}{\kappa_o}} \sqrt{\frac{\kappa_w^{\text{int}}}{\kappa_w}} \frac{\sqrt{\Gamma_o\Gamma_w}}{1 - \Gamma_o + \Gamma_w}, \quad (12g)$$

$$E_w = 2\sqrt{\frac{\kappa_w^{\text{int}}}{\kappa_w}} \sqrt{\frac{\kappa_w^{\text{in}}}{\kappa_w}} \frac{\Gamma_o - 1}{1 - \Gamma_o + \Gamma_w}, \quad (12h)$$

$$E_o = 2\sqrt{\frac{\kappa_o^{\text{int}}}{\kappa_o}} \sqrt{\frac{\kappa_o^{\text{in}}}{\kappa_o}} \frac{\Gamma_w + 1}{1 - \Gamma_o + \Gamma_w}. \quad (12i)$$

Furthermore, when the internal losses are negligible, i.e., $\kappa_j^{\text{int}}/\kappa_j^{\text{in}} \ll 1$, then we get $D_j = E_j \simeq 0$, and Eqs. (10a)–(10b) reduce to the simple forms presented in the paper,

$$\hat{d}_w = A_w \hat{c}_{w,\text{in}} - B \hat{c}_{o,\text{in}}^\dagger - C_w \hat{b}_{\text{int}}, \quad (13a)$$

$$\hat{d}_o = B \hat{c}_{w,\text{in}}^\dagger + A_o \hat{c}_{o,\text{in}} - C_o \hat{b}_{\text{int}}^\dagger, \quad (13b)$$

with coefficients given by

$$A_w = \frac{1 - (\Gamma_w + \Gamma_o)}{1 + \Gamma_w - \Gamma_o}, \quad (14a)$$

$$A_o = \frac{1 + (\Gamma_w + \Gamma_o)}{1 + \Gamma_w - \Gamma_o}, \quad (14b)$$

$$B = \frac{2\sqrt{\Gamma_w\Gamma_o}}{1 + \Gamma_w - \Gamma_o}, \quad (14c)$$

$$C_o = \frac{2i\sqrt{\Gamma_o}}{1 + \Gamma_w - \Gamma_o}, \quad (14d)$$

$$C_w = \frac{2i\sqrt{\Gamma_w}}{1 + \Gamma_w - \Gamma_o}. \quad (14e)$$

These input-output relations preserve the bosonic commutation relations, i.e., when the operators on the right in Eqs. (13a) and (13b) satisfy those commutation relations, we get $[\hat{d}_i, \hat{d}_j^\dagger] = \delta_{i,j}$ and $[\hat{d}_i, \hat{d}_j] = [\hat{d}_i^\dagger, \hat{d}_j^\dagger] = 0$, for $i, j \in w, o$.

IV. MICROWAVE-OPTICAL ENTANGLEMENT

A. Entanglement Metric

Equations (13a) and (13b) are driven by a collection of independent, thermal-state inputs, $\hat{c}_{w,\text{in}}$, $\hat{c}_{o,\text{in}}$, and \hat{b}_{int} and their adjoints. Consequently, those equations' outputs, \hat{d}_w and \hat{d}_o , are in a zero-mean, jointly-Gaussian state that is completely characterized by its non-zero second moments,

$$\bar{n}_w \equiv \langle \hat{d}_w^\dagger \hat{d}_w \rangle = |A_w|^2 \bar{n}_w^T + |B|^2 (\bar{n}_o^T + 1) + |C_w|^2 \bar{n}_b^T, \quad (15a)$$

$$\bar{n}_o \equiv \langle \hat{d}_o^\dagger \hat{d}_o \rangle = |B|^2 (\bar{n}_w^T + 1) + |A_o|^2 \bar{n}_o^T + |C_o|^2 (\bar{n}_b^T + 1), \quad (15b)$$

$$\langle \hat{d}_w \hat{d}_o \rangle = A_w B (\bar{n}_w^T + 1) - B A_o \bar{n}_o^T + C_w C_o (\bar{n}_b^T + 1). \quad (15c)$$

That joint state will be *classical*, i.e., have a proper P -representation, if and only if the phase-sensitive cross correlation, $|\langle \hat{d}_w \hat{d}_o \rangle|$, satisfies the classical bound [S5]

$$|\langle \hat{d}_w \hat{d}_o \rangle| \leq \sqrt{\bar{n}_w \bar{n}_o}. \quad (16)$$

When $|\langle \hat{d}_w \hat{d}_o \rangle|$ violates this bound, the microwave (w) and optical (o) modes are entangled. Note that, regardless of whether the *classical* bound is violated, the absence of phase-sensitive second moments in the joint state, viz., $\langle \hat{d}_w^2 \rangle = \langle \hat{d}_o^2 \rangle = 0$, implies that the reduced density operators for these individual modes are thermal states. The average photon numbers for the microwave and optical modes also put a *quantum* upper limit on $|\langle \hat{d}_w \hat{d}_o \rangle|$, given by [S6]

$$|\langle \hat{d}_w \hat{d}_o \rangle| \leq \sqrt{\max(\bar{n}_w, \bar{n}_o) [1 + \min(\bar{n}_w, \bar{n}_o)]}, \quad (17)$$

which can be saturated when $\bar{n}_w = \bar{n}_o$, but not when $\bar{n}_w \neq \bar{n}_o$.

Figure 2 in the main paper plots—versus Γ_w and Γ_o , and assuming experimentally-accessible parameter values—the entanglement metric

$$\mathcal{E} \equiv \frac{|\langle \hat{d}_w \hat{d}_o \rangle|}{\sqrt{\bar{n}_w \bar{n}_o}}, \quad (18)$$

which exceeds unity if and only if the microwave and optical modes are entangled. The entanglement metric provides a very simple entanglement criterion and, as we can see from the figure in the main paper, our microwave-optical source is proven to have wide regions of parameters where $\mathcal{E} > 1$.

B. Logarithmic Negativity and Coherent Information

Here we quantify the amount of entanglement generated by our microwave-optical source using standard measures in quantum information theory. In particular, we consider the log-negativity [S7] and the coherent information [S8], which are, respectively, an upper and a lower bound to the number of distillable entanglement bits (ebits) generated by the source. We normalize these measures by the mean number of microwave signal photons \bar{n}_w sent to the target. The rationale behind this normalization is physical and strictly connected with the specific model considered.

In fact, quantum illumination (QI) is a energy-constrained protocol, where quantum and classical sources are compared by fixing the mean number of photons in the signal mode [S9], which corresponds to the microwave mode in the present case. Thus, it is intuitively expected that, at fixed \bar{n}_w , the advantage of quantum illumination increases by increasing the amount of quantum entanglement (and more generally, quantum correlations) present in the source.

For this reason, the quality of the source can be estimated in two ways: (1) At fixed \bar{n}_w , we optimize the entanglement of the quantum source, or (2) we maximize the entanglement of the quantum source normalized by \bar{n}_w , i.e., the average entanglement carried by each microwave photon. The two options are clearly connected since, at fixed \bar{n}_w , the most entangled source is the one emitting more ebits per microwave photon. However, the second option is more flexible to use, since it can be applied to the cases where \bar{n}_w changes in terms of the various parameters of the problem, as it happens here on the cooperativity plane (Γ_o, Γ_w).

1. Logarithmic Negativity

In order to compute the log-negativity, we first determine the covariance matrix (CM) of our system in the frequency domain, which can be expressed as

$$\delta(\omega + \omega')V_{ij}(\omega) = \frac{1}{2}\langle u_i(\omega)u_j(\omega') + u_j(\omega')u_i(\omega) \rangle, \quad (19)$$

where

$$\mathbf{u}(\omega) = [X_w(\omega), Y_w(\omega), X_o(\omega), Y_o(\omega)]^T, \quad (20)$$

and $X_j = (d_j + d_j^\dagger)/\sqrt{2}$, $Y_j = (d_j - d_j^\dagger)/i\sqrt{2}$ with $j = o, w$. Note that the vacuum noise has variance 1/2 in these quadratures.

Now, by using Eqs. (13a), (13b) and (19), we obtain the CM for the quadratures of the microwave and optical cavities' outputs, which is given by the normal form

$$\mathbf{V}(\omega) = \begin{pmatrix} V_{11} & 0 & V_{13} & 0 \\ 0 & V_{11} & 0 & -V_{13} \\ V_{13} & 0 & V_{33} & 0 \\ 0 & -V_{13} & 0 & V_{33} \end{pmatrix}, \quad (21)$$

where we explicitly have

$$V_{11} = \frac{\langle X_w(\omega)X_w(\omega') \rangle}{\delta(\omega + \omega')} = \bar{n}_w + 1/2, \quad (22a)$$

$$V_{33} = \frac{\langle X_o(\omega)X_o(\omega') \rangle}{\delta(\omega + \omega')} = \bar{n}_o + 1/2, \quad (22b)$$

$$V_{13} = \frac{\langle X_w(\omega)X_o(\omega') + X_o(\omega')X_w(\omega) \rangle}{2\delta(\omega + \omega')} = \langle \hat{d}_w \hat{d}_o \rangle, \quad (22c)$$

and we have used the fact that $\langle \hat{d}_w \hat{d}_o \rangle$ is real valued. Note that Eq. (21) is the typical CM of a two-mode squeezed thermal state [S10].

The log-negativity E_N is given by [S7]

$$E_N = \max[0, -\log(2\zeta^-)], \quad (23)$$

where ζ^- is the smallest partially-transposed symplectic eigenvalue of $\mathbf{V}(\omega)$, given by [S11]

$$\zeta^- = 2^{-1/2} \left(V_{11}^2 + V_{33}^2 + 2V_{13}^2 - \sqrt{(V_{11}^2 - V_{33}^2)^2 + 4V_{13}^2(V_{11} + V_{33})^2} \right)^{1/2}. \quad (24)$$

In Fig. 2 of the main paper, we have plotted the normalized log-negativity E_N/\bar{n}_w versus the cooperativities, Γ_w and Γ_o . From panel (b) of that figure, we can see the presence of a wide region where the quality of the source is very good in terms of ebits of log-negativity per microwave photon emitted.

It is easy to show that $E_N = 0$ for $\mathcal{E} \leq 1$. Moreover, for the case of interest for QI—in which $\bar{n}_j \equiv \langle \hat{d}_j^\dagger \hat{d}_j \rangle \leq 1$ for $j = w, o$ —we find that $2\zeta^-$ decreases monotonically, at fixed \bar{n}_w and \bar{n}_o , as $|\langle \hat{d}_w \hat{d}_o \rangle|$ increases from zero to its quantum upper bound from Eq. (17). Thus, given $\bar{n}_j \leq 1$ for $j = w, o$, the logarithmic negativity E_N for our source can be related with the entanglement metric \mathcal{E} .

2. Coherent Information

Here we compute the coherent information associated with our microwave-optical source. This is given by [S8]

$$I(o)w = S(w) - S(o, w), \quad (25)$$

where $S(w)$ is the von Neumann entropy [S11] of the microwave mode, while $S(o, w)$ is the joint von Neumann entropy of the optical and microwave modes. As mentioned before, this provides a lower bound to the number of ebits which

are distillable from the source. In fact, according to the hashing inequality [S12], $I(o|w)$ gives the distillation rate (ebits per use of the source) which is achievable by distillation protocols based on one-way classical communication (here directed from the optical to the microwave part).

For a Gaussian state, like our source, we can simply express the entropic terms in Eq. (25) in terms of the symplectic eigenvalue ν_w of the reduced CM associated with the microwave mode and the symplectic spectrum $\{\nu_-, \nu_+\}$ of the global CM $\mathbf{V}(\omega)$ associated with the microwave and optical modes. These eigenvalues are given by $\nu_w = V_{11}$ and [S11]

$$\nu_{\pm} = 2^{-1/2} \left(V_{11}^2 + V_{33}^2 - 2V_{13}^2 \pm \sqrt{(V_{11}^2 - V_{33}^2)^2 - 4V_{13}^2(V_{11} - V_{33})^2} \right)^{1/2}. \quad (26)$$

Thus, we have [S11]

$$I(o|w) = h(V_{11}) - h(\nu_-) - h(\nu_+), \quad (27)$$

where [S13]

$$h(x) \equiv \left(x + \frac{1}{2}\right) \log_2 \left(x + \frac{1}{2}\right) - \left(x - \frac{1}{2}\right) \log_2 \left(x - \frac{1}{2}\right). \quad (28)$$

In Fig. 2 of the main paper, we have plotted the normalized coherent information $I(o|w)/\bar{n}_w$ versus the cooperativities, Γ_w and Γ_o . From panel (c) of that figure, we can see the presence of a wide region where the quality of the source is good in terms of qubits of coherent information per microwave photon emitted (lower bound to the number of ebits per microwave photon). Finally, note that the computation of the normalized *reverse* coherent information [S14, S15] $I(o\langle w)/\bar{n}_w$ (where the direction of the classical communication is inverted from the microwave to the optical part) leads to completely similar results, as shown in Fig. 5.

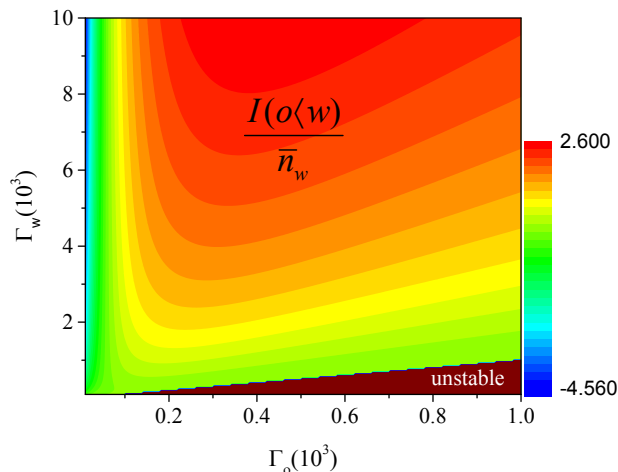


FIG. 5. Normalized reverse coherent information $I(o\langle w)/\bar{n}_w$ (qubits per microwave photon) plotted on the cooperativity plane (Γ_o, Γ_w) . See Fig. 2 of the main paper for the other parameter values.

V. MICROWAVE-OPTICAL QUANTUM CORRELATIONS BEYOND ENTANGLEMENT

Our microwave-optical source generates a Gaussian state which is mixed, as one can easily check from the numerical values of its von Neumann entropy $S(o,w)$. It is therefore important to describe its quality also in terms of general quantum correlations beyond quantum entanglement. Thus we compute here the quantum discord [S16] of the source $D(w|o)$, capturing the basic quantum correlations which are carried by the microwave mode sent to target. Such quantity is normalized by \bar{n}_w , for the same reasons we have previously explained for quantum entanglement: The best sources for our QI problem are expected to be those maximizing the amount of quantum correlations per microwave photon emitted.

Since our source emits a mixed Gaussian state which is a two-mode squeezed thermal state, we can compute its (unrestricted) quantum discord using the formulas of Ref. [S10]. In particular, the CM in Eq. (21) can be expressed as [S10]

$$\mathbf{V}(\omega) = \begin{pmatrix} (\tau b + \eta)\mathbf{I} & \sqrt{\tau(b^2 - 1)}\mathbf{Z} \\ \sqrt{\tau(b^2 - 1)}\mathbf{Z} & b\mathbf{I} \end{pmatrix}, \quad \mathbf{I} \equiv \text{diag}(1, 1), \quad \mathbf{Z} \equiv \text{diag}(1, -1), \quad (29)$$

where

$$b = V_{33}, \quad \tau = \frac{V_{13}^2}{V_{33}^2 - 1}, \quad \eta = V_{11} - \frac{V_{33}V_{13}^2}{V_{33}^2 - 1}. \quad (30)$$

Thus, we may write [S10]

$$D(w|o) = h(b) - h(\nu_-) - h(\nu_+) + h(\tau + \eta) \quad (31)$$

$$= h(V_{33}) - h(\nu_-) - h(\nu_+) + h \left[V_{11} + \frac{V_{13}^2(1 - V_{33})}{V_{33}^2 - 1} \right], \quad (32)$$

where ν_- and ν_+ are the symplectic eigenvalues of $\mathbf{V}(\omega)$.

In Fig. 2 of the main paper, we have plotted the normalized quantum discord $D(w|o)/\bar{n}_w$ versus the cooperativities, Γ_w and Γ_o . From panel (d) of that figure, we can see the presence of a wide region where the quality of the source is very good in terms of discordant bits per microwave photon emitted. Furthermore, the similarity between this normalized measure and the final QI advantage (figure 4 of the main paper) is remarkable.

Finally, note that the computation of the normalized version of the other quantum discord [S16] $D(o|w)/\bar{n}_w$ leads to similar results, as shown below in Fig. 6 of this Supplemental Material.

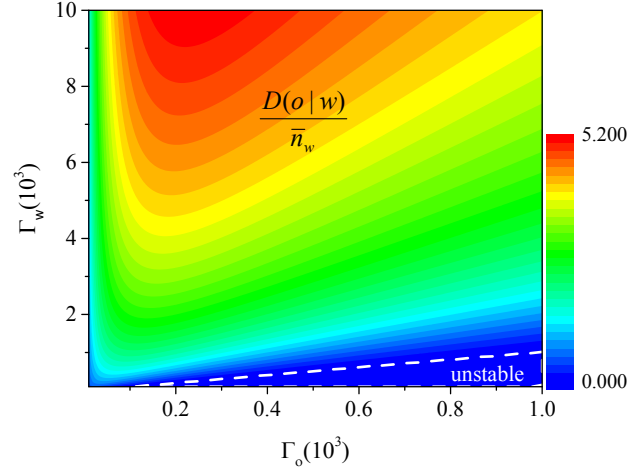


FIG. 6. Normalized quantum discord $D(o|w)/\bar{n}_w$ (discordant bits per microwave photon) plotted on the cooperativity plane (Γ_o, Γ_w) . See Fig. 2 of the main paper for the other parameter values.

VI. ERROR PROBABILITY FOR M MODE PAIRS

Our transmitter's EOM converter is governed by Eqs. (13a) and (13b) in which the coefficients appearing therein are as specified in Eqs. (14a)–(14e). These same coefficients appear in the input-output relation

$$\hat{d}_{\eta,o} = B\hat{c}_R^\dagger + A_o\hat{c}'_{o,\text{in}} - C_o\hat{b}'_{\text{int}}^\dagger, \quad (33)$$

for the QI receiver's EOM converter. Equations (13a) and (13b) apply to one of the $M = t_m W_m \gg 1$ independent, identically-distributed (iid) mode pairs produced by the bandwidth- W_m , continuous-wave transmitter during the t_m -sec-duration measurement interval used to discriminate target absence from target presence. Under either hypothesis

(target absent or present), the QI receiver takes as its inputs M iid mode pairs, $\{\hat{c}_R^{(k)}, \hat{d}_o^{(k)} : 1 \leq k \leq M\}$ that are in a zero-mean, jointly-Gaussian state characterized by the conditional (given target absence or presence) second moments: $\langle \hat{c}_R^{(k)\dagger} \hat{c}_R^{(k)} \rangle_{H_j}$, $\langle \hat{d}_o^{(k)\dagger} \hat{d}_o^{(k)} \rangle_{H_j}$, and $\langle \hat{c}_R^{(k)} \hat{d}_o^{(k)} \rangle_{H_j}$. The receiver's EOM converter transforms the returned microwave modes, $\hat{c}_R^{(k)}$, into optical modes, $\hat{d}_{\eta,o}^{(k)}$, such that the $\{\hat{d}_{\eta,o}^{(k)}, \hat{d}_o^{(k)} : 1 \leq k \leq M\}$ are iid mode pairs which, under either hypothesis, are in a zero-mean jointly-Gaussian state characterized by the second moments $\langle \hat{d}_{\eta,o}^{(k)\dagger} \hat{d}_{\eta,o}^{(k)} \rangle_{H_j}$, $\langle \hat{d}_o^{(k)\dagger} \hat{d}_o^{(k)} \rangle_{H_j}$, and $\langle \hat{d}_{\eta,o}^{(k)} \hat{d}_o^{(k)} \rangle_{H_j}$. Note that, in addition to its transforming the microwave modes into optical modes, the EOM converter transforms the *phase-sensitive* cross correlations, $\{\langle \hat{c}_R^{(k)} \hat{d}_o^{(k)} \rangle_{H_1}\}$, into *phase-insensitive* cross correlations, $\{\langle \hat{d}_{\eta,o}^{(k)} \hat{d}_o^{(k)} \rangle_{H_1}\}$, which can be measured—as shown in Fig. 7—by mixing returned and retained modes on a 50–50 beam splitter whose outputs are

$$\hat{a}_{\eta,\pm}^{(k)} \equiv \frac{\hat{d}_{\eta,o}^{(k)} \pm \hat{d}_o^{(k)}}{\sqrt{2}}. \quad (34)$$

These modes are then photodetected, yielding modal photon-counts that are equivalent to measurements of the number operators $\hat{N}_{\eta,\pm}^{(k)} \equiv \hat{a}_{\eta,\pm}^{(k)\dagger} \hat{a}_{\eta,\pm}^{(k)}$. Finally, the target absence-or-presence decision is made by comparing the difference of the two detectors' total photon counts [S17], which is equivalent to the quantum measurement

$$\hat{N}_\eta = \sum_{k=1}^M \left(\hat{N}_{\eta,+}^{(k)} - \hat{N}_{\eta,-}^{(k)} \right), \quad (35)$$

with a threshold chosen to make the receiver's false-alarm probability

$$P_F \equiv \Pr(\text{decide target present} \mid \text{target absent}), \quad (36)$$

equals its miss probability,

$$P_M \equiv \Pr(\text{decide target absent} \mid \text{target present}). \quad (37)$$

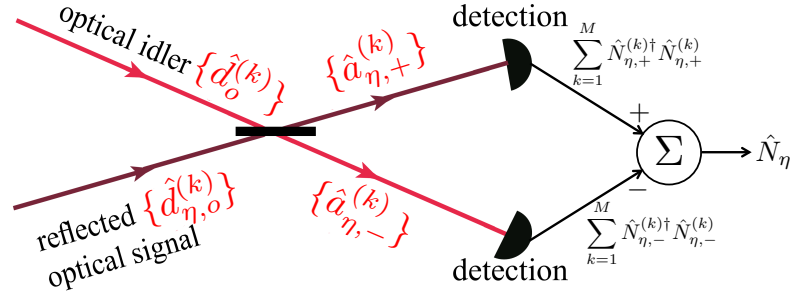


FIG. 7. Optical post-processing in the QI receiver. A 50-50 beam splitter mixes the wavelength-converted return modes $\{\hat{d}_{\eta,o}^{(k)}\}$, from the receiver's EOM converter with the retained idler modes, $\{\hat{d}_o^{(k)}\}$. The beam splitter's outputs are detected, yielding classical outcomes equivalent to the quantum measurements $\sum_{k=1}^M \hat{N}_{\eta,\pm}^{(k)}$, and the difference of these outputs, equivalent to the quantum measurement of \hat{N}_η , is used as the input to a threshold detector (not shown) whose output is the target absence or presence decision.

Because QI employs an enormous number of mode pairs, and those mode pairs are iid under both hypotheses, the Central Limit Theorem implies that the \hat{N}_η measurement yields a random variable that is Gaussian, conditioned on target absence or target presence. It follows that the QI receiver's error probability, for equally-likely hypotheses, satisfies

$$P_{\text{QI}}^{(M)} = \frac{P_F + P_M}{2} = \frac{\text{erfc}\left(\sqrt{\text{SNR}_{\text{QI}}^{(M)}/8}\right)}{2}, \quad (38)$$

where the M -mode signal-to-noise ratio is

$$\text{SNR}_{\text{QI}}^{(M)} = \frac{4(\langle \hat{N}_\eta \rangle_{H_1} - \langle \hat{N}_\eta \rangle_{H_0})^2}{\left(\sqrt{\langle \Delta \hat{N}_\eta^2 \rangle_{H_0}} + \sqrt{\langle \Delta \hat{N}_\eta^2 \rangle_{H_1}}\right)^2}, \quad (39)$$

with $\langle \hat{N}_\eta \rangle_{H_j}$ and $\langle \Delta \hat{N}_\eta^2 \rangle_{H_j}$, for $j = 0, 1$, being the conditional means and conditional variances of \hat{N}_η .

The iid nature of the $\{\hat{N}_{\eta,+}^{(k)}, \hat{N}_{\eta,-}^{(k)}\}$ allow us to rewrite the M -mode SNR in terms of single-mode moments, i.e.,

$$\text{SNR}_{\text{QI}}^{(M)} = \frac{4M[(\langle \hat{N}_{\eta,+} \rangle_{H_1} - \langle \hat{N}_{\eta,-} \rangle_{H_1}) - (\langle \hat{N}_{\eta,+} \rangle_{H_0} - \langle \hat{N}_{\eta,-} \rangle_{H_0})]^2}{\left(\sqrt{\langle (\Delta \hat{N}_{\eta,+} - \Delta \hat{N}_{\eta,-})^2 \rangle_{H_0}} + \sqrt{\langle (\Delta \hat{N}_{\eta,+} - \Delta \hat{N}_{\eta,-})^2 \rangle_{H_1}} \right)^2}, \quad (40)$$

where we have suppressed the superscript (k) . The moments needed to instantiate Eq. (40) are now easily found. In particular, for the mean values we find that

$$\langle \hat{N}_{\eta,\pm} \rangle_{H_0} = |B|^2[(\bar{n}_B + \bar{n}_w^T)/2 + 1] + |A_o|^2 \bar{n}_o^T + |C_o|^2(\bar{n}_b^T + 1), \quad (41a)$$

$$\begin{aligned} \langle \hat{N}_{\eta,\pm} \rangle_{H_1} &= \langle \hat{N}_{\eta,\pm} \rangle_{H_0} + \eta |B|^2[|A_w|^2(\bar{n}_w^T + 1) + |B|^2 \bar{n}_o^T + |C_w|^2(\bar{n}_b^T + 1)]/2 \\ &\quad \pm \sqrt{\eta} \text{Re}[|B|^2 A_w(\bar{n}_w^T + 1) - |B|^2 A_o \bar{n}_o^T + B^* C_w C_o(\bar{n}_b^T + 1)] \end{aligned} \quad (41b)$$

whence

$$\langle \hat{N}_{\eta,+} \rangle_{H_0} - \langle \hat{N}_{\eta,-} \rangle_{H_0} = 0, \quad (42a)$$

$$\langle \hat{N}_{\eta,+} \rangle_{H_1} - \langle \hat{N}_{\eta,-} \rangle_{H_1} = 2\sqrt{\eta} \text{Re}[|B|^2 A_w(\bar{n}_w^T + 1) - |B|^2 A_o \bar{n}_o^T + B^* C_w C_o(\bar{n}_b^T + 1)], \quad (42b)$$

For the variances we get [S18]

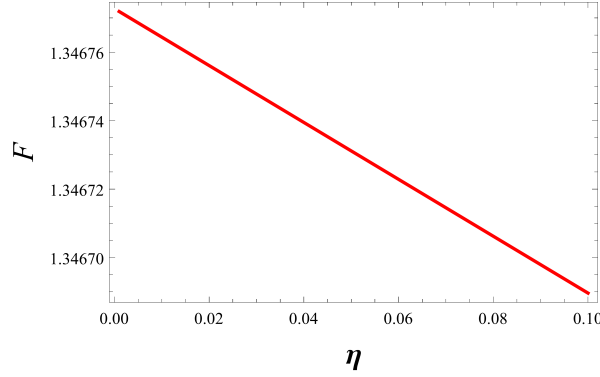


FIG. 8. The dependence of the QI-advantage figure of merit $\mathcal{F} \equiv \text{SNR}_{\text{QI}}^{(M)}/\text{SNR}_{\text{coh}}^{(M)}$ on η . See Fig. 2 of the main paper for the other parameter values.

$$\langle (\Delta \hat{N}_{\eta,+} - \Delta \hat{N}_{\eta,-})^2 \rangle_{H_j} = \langle \hat{N}_{\eta,+} \rangle_{H_j} (\langle \hat{N}_{\eta,+} \rangle_{H_j} + 1) + \langle \hat{N}_{\eta,-} \rangle_{H_j} (\langle \hat{N}_{\eta,-} \rangle_{H_j} + 1) - (\langle \hat{d}_{\eta,o}^\dagger \hat{d}_{\eta,o} \rangle_{H_j} - \langle \hat{d}_o^\dagger \hat{d}_o \rangle)^2/2, \quad (43)$$

for $j = 0, 1$, where

$$\langle \hat{d}_{\eta,o}^\dagger \hat{d}_{\eta,o} \rangle_{H_j} = \begin{cases} |B|^2(\bar{n}_B + 1) + |A_o|^2 \bar{n}_o^T + |C_o|^2(\bar{n}_b^T + 1), & \text{for } j = 0 \\ \langle \hat{d}_{\eta,o}^\dagger \hat{d}_{\eta,o} \rangle_{H_0} + \eta |B|^2[|A_w|^2(\bar{n}_w^T + 1) + |B|^2 \bar{n}_o^T + |C_w|^2(\bar{n}_b^T + 1)], & \text{for } j = 1. \end{cases} \quad (44)$$

It is interesting to see how the transmitter-to-target-to-receiver transmissivity, η , affects QI's performance advantage over coherent-state operation. Figure 8 shows the dependence of the QI-advantage figure of merit $\mathcal{F} \equiv \text{SNR}_{\text{QI}}^{(M)}/\text{SNR}_{\text{coh}}^{(M)}$ for $10^{-3} \leq \eta \leq 10^{-1}$. We have restricted our attention here to the low- η regime, because we follow the lead of [S9] in assuming that the target's presence has no passive signature. A passive signature—a lower received background level in the presence of the target—would permit the target to be detected without transmitting any microwave radiation. We preclude that possibility by assuming that the noise mode \hat{c}_B has average photon number \bar{n}_B when the target is absent and average photon number $\bar{n}_B/(1 - \eta)$ when the target is present. Unless $\eta \ll 1$, so that these two average photon numbers are nearly the same, this assumption is physically unreasonable.

[S1] R. W. Andrews, R. W. Peterson, T. P. Purdy, K. Cicak, R. W. Simmonds, C. A. Regal, and K. W. Lehnert, Nature Phys. **10**, 321 (2014).

- [S2] J. Bochmann, A. Vainsencher, D. D. Awschalom, and A. N. Cleland, *Nature Phys.* **9**, 712 (2013).
- [S3] T. Bagci, A. Simonsen, S. Schmid, L. G. Villanueva, E. Zeuthen, J. Appel, J. M. Taylor, A. Sørensen, A. Schliesser, and E. S. Polzik, *Nature* **507**, 81 (2014).
- [S4] Sh. Barzanjeh, D. Vitali, P. Tombesi, and G. J. Milburn, *Phys. Rev. A* **84**, 042342 (2011).
- [S5] The classical bound arises from the requirement that $\langle |xd_w + d_o^*|^2 \rangle \geq 0$ for classical, complex-valued random variables d_w and d_o , where $\langle \cdot \rangle$ denotes classical ensemble average and x is an arbitrary real-valued parameter.
- [S6] The quantum bound arises from the requirement that $\langle (x\hat{d}_w + \hat{d}_o^\dagger)(x\hat{d}_w + \hat{d}_o^\dagger) \rangle \geq 0$ and $\langle (x\hat{d}_o + \hat{d}_w^\dagger)(x\hat{d}_o + \hat{d}_w^\dagger) \rangle \geq 0$, where x is an arbitrary real-valued parameter.
- [S7] J. Eisert, Ph.D. thesis, University of Potsdam, 2001; G. Vidal and R. F. Werner, *Phys. Rev. A* **65**, 032314 (2002); M.B. Plenio, *Phys. Rev. Lett.* **95**, 090503 (2005).
- [S8] B. Schumacher, and M. A. Nielsen, *Phys. Rev. A* **54**, 2629 (1996); S. Lloyd, *Phys. Rev. A* **55**, 1613 (1997).
- [S9] S.-H. Tan, B. I. Erkmen, V. Giovannetti, S. Guha, S. Lloyd, L. Maccone, S. Pirandola, and J. H. Shapiro, *Phys. Rev. Lett.* **101**, 253601 (2008).
- [S10] S. Pirandola, G. Spedalieri, S. L. Braunstein, N. J. Cerf, and S. Lloyd, *Phys. Rev. Lett.* **113**, 140405 (2014).
- [S11] C. Weedbrook, S. Pirandola, R. García-Patrón, N. J. Cerf, T. C. Ralph, J. H. Shapiro, and S. Lloyd, *Rev. Mod. Phys.* **84**, 621 (2012).
- [S12] I. Devetak, and A. Winter, *Proc. R. Soc. Lond. A* **461**, 207 (2005).
- [S13] Note that the expression of the entropic function $h(x)$ is that for vacuum noise equal to $1/2$. Our notation is different from that of Ref. [S11], where the vacuum noise is equal to 1.
- [S14] R. García-Patrón, S. Pirandola, S. Lloyd, and J. H. Shapiro, *Phys. Rev. Lett.* **102**, 210501 (2009).
- [S15] S. Pirandola, R. García-Patrón, S. L. Braunstein, and S. Lloyd, *Phys. Rev. Lett.* **102**, 050503 (2009).
- [S16] K. Modi, A. Brodutch, H. Cable, T. Paterek, and V. Vedral, *Rev. Mod. Phys.* **84**, 1655 (2012).
- [S17] For continuous-wave operation with a t_m -sec-long measurement interval, the \hat{N}_η measurement is realized by the photon-count difference between the two detectors over that measurement interval.
- [S18] S. Guha and B. I. Erkmen, *Phys. Rev. A* **80**, 052310 (2009).